# Rotational Excitation in the $N_2(C^3\Pi_u)$ and $N_2^+(B^2\Sigma_u^+)$ States Produced by Electron Impact of $N_2$

Ikuo TOKUE,* Jundong WANG, † and Yoshio ITO
Department of Chemistry, Faculty of Science, Niigata University, Ikarashi, Niigata 950-21
(Received August 28, 1992)

Rotational state distributions of $N_2(C^3\Pi_u)$ and $N_2^+(B^2\Sigma_u^+)$ produced by electron impact on $N_2$ have been measured by observing the 0–0 band of the $N_2(C^3\Pi_u—B^3\Pi_g)$ and $N_2^+(B^2\Sigma_u^+—^2\Sigma_g^+)$ emissions, respectively. The average rotational quantum number for $N_2(C)$ decreases with increasing impact energy up to 30 eV (so-called rotational excitation), reaches a minimum, and increases with impact energy above 45 eV. The rotational excitation has been observed in formation of $N_2(C)$ for the first time. This trend indicates the importance of multipole interactions between the target $N_2$ molecule and the incident electron.

Rotational state distributions of diatomic and triatomic ions produced by electron-impact excitation have been studied extensively by monitoring fluorescences from excited states. For thermodynamical studies of expansion mechanism in supersonic free jet, the $N_2^+(B^2\Sigma_u^+—X^2\Sigma_g^+)$ emission stimulated by electron impact was used to estimate the original rotational distribution of $N_2$ under various flow conditions.[1—3] Many data on the rotational distribution of the $N_2^+(B^2\Sigma_u^+)$ ion have been accumulated because of the interest in the possibility of rotational excitation in simultaneous ionization-excitation of $N_2$.[4—6] The general features of rotational excitation thus revealed are as follows: (1) the rotational distributions are non-Boltzmann with a large population in the lowest few rotational levels followed by a long tail to higher rotational levels, and (2) the rotational energy of the product ion increases sharply with decreasing the energy of impinging electrons.

The observed trend was first interpreted qualitatively by an idea that the rotational excitation is caused by a combination of angular momentum transfer through multipole interactions between the incident electron and the target $N_2$ molecule and through those between the scattered and ejected electrons and the product $N_2^+$ ion.[7] Nevertheless, the details of experimental results and their interpretations have not always been consistent with each other.[8,9]

In order to clarify the rotational selection rule electron-impact ionization-excitation of CO was investigated at 150—900 eV and deviations from the electric dipole selection rule were observed below 200 eV from the analysis of the $CO^+(A^2\Pi—X^2\Sigma^+)$ emission.[10] A similar trend of rotational excitation has been also observed in the $N_2^+(X^2\Sigma_g^+)$ and $CO_2^+(\tilde{X}^2\Pi_g)$ states by laser-induced fluorescence (LIF).[8,11—16]

As for the theoretical treatment, the cross section of the pure rotational transition stimulated by collisions with slow electrons was first derived by Gerjuoy and Stein[17] for homonuclear molecules ($H_2$ and $N_2$) which possess no permanent dipole. Whereas, no adequate theoretical treatment of the transfer of angular momentum by electron-molecule collision exists when it includes simultaneous ionization-excitation. For the present, experimental results are the only way of understanding such phenomena.

In a previous study,[18] trends of rotational excitation have been observed in $N_2O^+(\tilde{A}^2\Sigma^+)$, $CO_2^+(\tilde{A}^2\Pi_u)$, and $CS_2^+(\tilde{A}^2\Pi_u)$ produced by electron-impact ionization. From the dependence of the rotational distributions on impact energy, we have pointed out the importance of angular momentum transfer through the quadrupole interaction between the scattered and ejected electrons and the residual ion. The trend of rotational excitation seems to have general possibility so that one can expect to observe similar rotational excitations in other states. Such an experiment for other states, especially for neutral states, can provide further information about interactions between electrons and target molecules. To our knowledge, there has however been only a very little amount of information about the dependence of rotational distributions for neutral states on impact energy. In this context, rotational distributions of the $N_2(C^3\Pi_u—B^3\Pi_g)$ emission stimulated by electron impact have been analyzed up to 100 eV and the results have been compared with those for the $N_2^+(B^2\Sigma_u^+—X^2\Sigma_g^+)$ emission. A similar trend of rotational excitation has been observed in $N_2(C)$ below 30 eV for the first time. The rotational distributions obtained above 45 eV indicate that secondary processes via collisions of target molecules with scattered electrons mainly contribute to formation of $N_2(C)$. The dependence of rotational distribution of $N_2(C)$ on the impact energy implies the importance of multipole interactions between the incident electron and the target molecule.

## Experimental

The crossed free jet/electron beam apparatus and experimental details have been described previously.[19] In brief, the supersonic free jet was produced by expanding $N_2$ gas into a collision chamber through a pulsed nozzle (0.1 mm diameter). $N_2$ gas was expanded with a stagnation pressure of 300 kPa (3 atm). The nozzle was pulsed at a repetition frequency of 10 Hz and each pulse lasted 4—6 ms. The am-

† On leave from Department of Chemistry, Heilonjiang University, Harbin, China.

bient pressure at the collision chamber was kept at 42—61 mPa and the electron beam source was evacuated to 3 mPa. The free jet crossed an electron beam perpendicularly 1.5 cm downstream from the nozzle.

The impact energy of the electron beam was controlled from the threshold up to 300 eV and the beam current was suppressed in the 15—30 μA range to avoid the influence of secondary electrons. The energy of impinging electrons was calibrated against the appearance potentials of the $N_2(C^3\Pi_u—B^3\Pi_g)$ and $N_2^+(B^2\Sigma_u^+—X^2\Sigma_g^+)$ emissions.[20] When the impact energy was decreased below 60 eV, the convergence of the electron beam was diffused by mutual repulsion between electrons. Therefore, a Helmholz coil was used to provide an external magnetic field about 3 mT (30 gauss) along the beam axis in order to maintain the beam shape.

Fluorescence produced by the electron-impact excitation was observed in a direction perpendicular to both the molecular and electron beams. The optical path was carefully baffled by placing a diaphram next to the window in order to reduce fluorescence from targets near the shock barrel. Moreover, to eliminate the emission from thermalized molecules near the beam center, the emission intensity obtained at the nozzle-off period was subtracted from that obtained at the nozzle-on period.

## Results

The 0–0 bands of the $N_2(C^3\Pi_u— B^3\Pi_g)$ and $N_2^+(B^2\Sigma_u^+—X^2\Sigma_g^+)$ emissions have been measured in order to determine rotational populations of the $N_2(C^3\Pi_u)$ and $N_2^+(B^2\Sigma_u^+)$ states. Figures 1 and 2 show typical emission spectra of the 0–0 band of the $N_2$(C–B) and $N_2^+$(B–X) systems, respectively, produced by electron impact comparing with the synthetic spectra. Although the spectral resolution is inadequate to resolve each rotational line, it becomes evident that the relative intensities vary with the impact energy. The rotational distributions of $N_2$(C) and $N_2^+$(B) have been derived from the observed spectra by a band-envelope simulation: the observed spectrum was compared with the synthetic spectrum, which was obtained by convolution of the calculated intensities with the slit function. This function was evaluated by a helium line at 501.57 nm measured under the same optical condition.

**Rotational Distribution of $N_2$(C).** The emission intensity $I_{J'J''}$ (photon counts/s) of the $J'$-$J''$ rotational line for the $N_2(C^3\Pi_u—B^3\Pi_g)$ system is given by[21]

$$I_{J'J''} = C_1 \nu_{J'J''}^3 S_{J'J''} P(J')/g_{J'}, \quad (1)$$

where $C_1$ is a constant in the present treatment, $\nu_{J'J''}$ is the transition frequency, and $S_{J'J''}$ is the line strength. The $P(J')$ and $g_{J'}$ $(=2J'+1)$ are the rotational population and the statistical weight, respectively, of the $J'$ level.

For the $C^3\Pi_u$ and $B^3\Pi_g$ states of $N_2$, a gradual transition from Hund's coupling case (a) to case (b) takes place at higher rotational levels. The line strengths were calculated by using the formulas given by Budó.[22] Thirteen branches were used for band envelope analysis. Among them three P and R branches are strong. For the six strong branches the observed transition frequencies[23,24] were used, whereas the frequencies calculated from the spectroscopic constants[20] were used for the other weak branches.

The observed spectrum was compared with the best-fit synthetic band envelope as shown in Fig. 1; the residual of the intensity at the wavelength $\lambda_i$ is given by

$$\Delta I(\lambda_i) = I_o(\lambda_i) - f I_s(\lambda_i), \quad (2)$$

where $I_o$ and $I_s$ represent the observed and synthetic intensities, respectively, and $f$ is chosen such that the summation of the residual taken over all $\lambda_i$ equals zero. The root-mean-square value of the residual was used as a criterion of the fit.

For the $N_2$(C–B) system, the band envelope analysis has mainly applied to the R branches in the 336.1—336.9 nm region because of heavy overlapping among the P branches. Rotational populations for $J'$ up to 14 of $N_2$(C) thus obtained are shown in Fig. 3; $P(J')/g_{J'}$ corresponds to the $I_{J'J''}/\nu^3 S_{J'J''}$ value in the procedure in which rotational lines are fully resolved. Rotational distributions of lower levels ($J' \leqq 7$) obtained at 14, 20, and 30 eV are nearly represented by Boltzmann temperatures of 52, 44, and 44 K, respectively, whereas the populations for $J'$ above 8 are overpopulated.

**Rotational Distribution of $N_2^+$(B).** The emission intensity of the $N'$-$N''$ rotational line in the $N_2^+(B^2\Sigma_u^+—X^2\Sigma_g^+)$ system is also represented by Eq. 1 but replacing the rotational quantum numbers $J'$ and $J''$ by $N'$ and $N''$, respectively. The $B^2\Sigma_u^+$ and $X^2\Sigma_g^+$ states belong Hund's case (b) so that there are six branches. Among them two P and R branches are strong and two Q branches are weak. The line strengths were calculated by Höln-London formulas.[21] The observed transition frequencies[25] were used for the P and P branches, whereas for the Q branches the frequencies calculated from the spectroscopic constants[20] were used.

Rotational populations for $N'$ up to 19 of $N_2^+$(B) thus obtained are shown in Fig. 4. The rotational distributions of lower levels ($N' \leqq 4$) obtained at 30, 45, and 100 eV are nearly represented by Boltzmann temperatures of 35, 30, and 25 K, respectively, whereas the populations for $N'$ above 5 are overpopulated. This tendency is the same as that of $N_2^+$(X) reported by Nagata et al.[14] irrespective of the difference in the experimental conditions.

## Discussion

**Nascent Rotational Distributions.** The rotational distributions of $N_2$(C) and $N_2^+$(B) obtained in the present experiment represent the nascent distributions if the following processes are ignored: (1) collisional relaxation, (2) radiative cascading from higher excited states, (3) formation of $N_2$(C) and $N_2^+$(B) via secondary

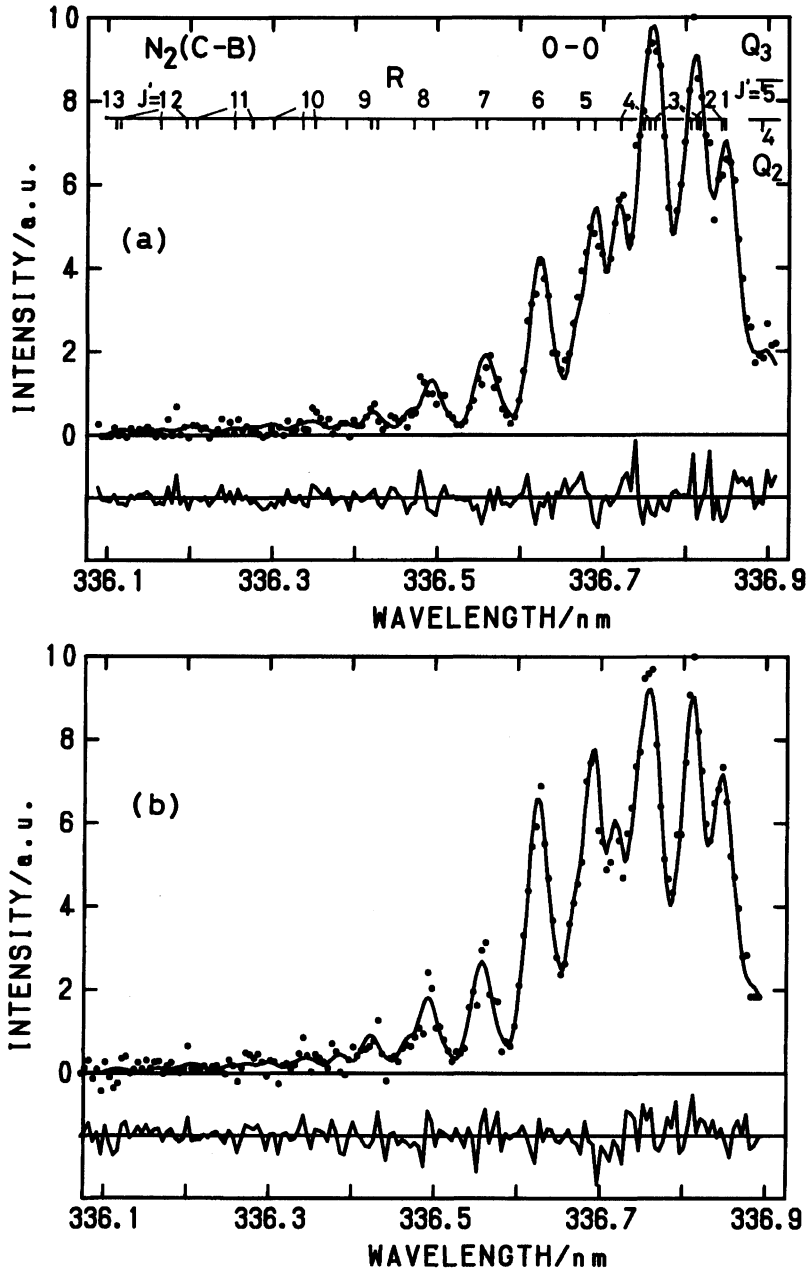


Fig. 1. Observed emission spectra (dots) of the $N_2(C^3\Pi_u—B^3\Pi_g)$ system produced at impact energies of (a) 30 eV and (b) 14 eV with the 0.028 nm fwhm resolution; the trace (upper part) is the best-fit synthetic spectrum and the residual (see text) is also shown.

processes.

(1) The frequencies of collisions that the emitters suffer under the present experimental conditions are estimated to be $2\times10^3$ $s^{-1}$ from the theoretical data[26] on the assumption of a hard sphere collision cross section of $1\times10^{-19}$ $m^2$. The collisional probabilities of $N_2(C)$ and $N_2^+(B)$ during their lifetimes are estimated to be $10^{-4}$ and $2\times10^{-4}$, respectively, in comparison with the fluorescence lifetime of $N_2(C)$ 35—41 ns and that of $N_2^+(B)$ 60.5 ns.[20] Hence, collisional relaxations of $N_2(C)$ and $N_2^+(B)$ are negligible.

(2) Electron-impact excitation of $N_2$ at impact energies above 14 eV can produce many higher states in addition to the $C^3\Pi_u$ state. Nevertheless, radiative cascadings from higher excited states to the C state are not known.[20] For $N_2^+$, one of the K state produced above 395 eV by removal of one K electron is known to cascade to the $B^2\Sigma_u^+$ state.[20] Thus, the contamination due to the cascading is insignificant in the electron impact below 300 eV.

(3) Secondary electron effects on formation of $N_2(C)$ were studied by Borst and Imami.[27,28] They have concluded that secondary slow electrons play an appreciable role at pressures of 13.3 mPa or higher. In such

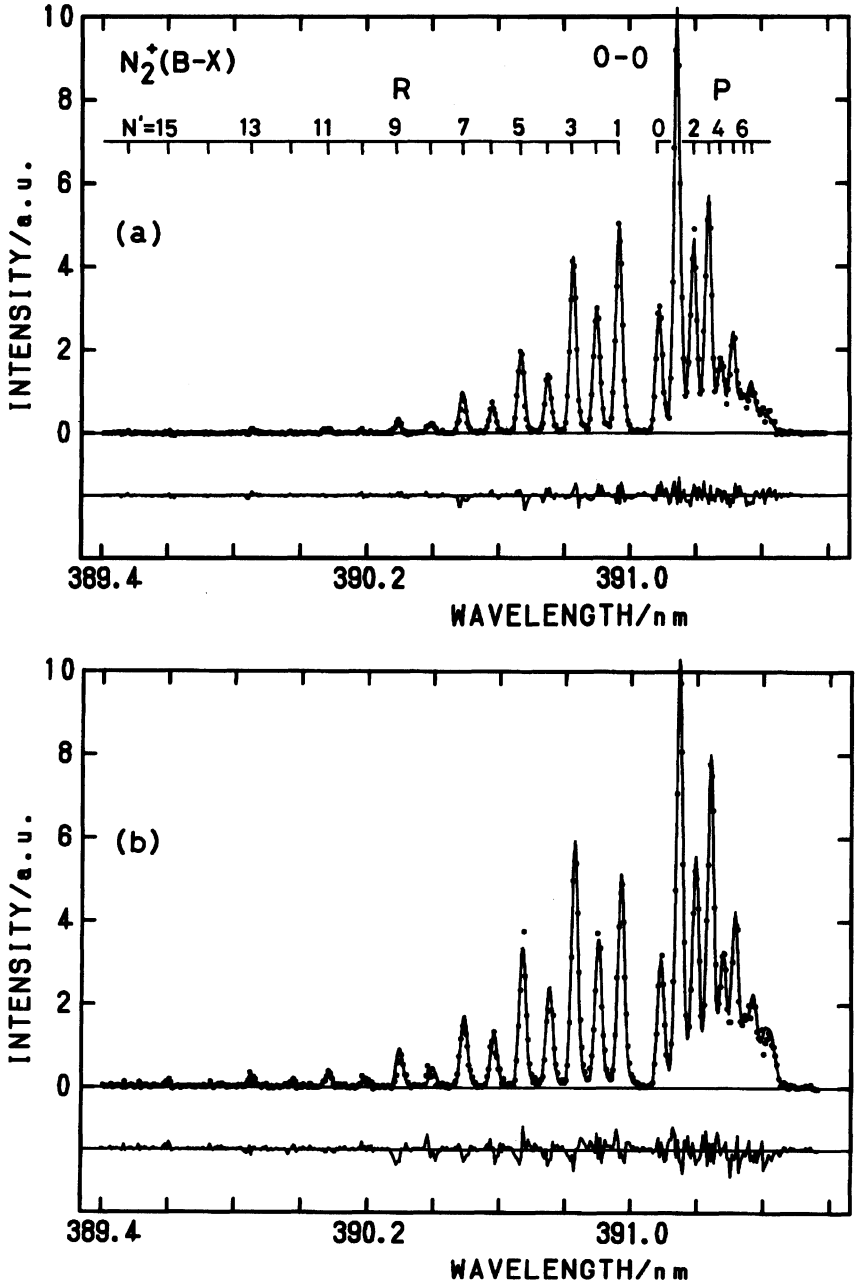


Fig. 2. Observed emission spectra (dots) of the $N_2^+(B^2\Sigma_u^+—X^2\Sigma_g^+)$ system produced at impact energies of (a) 100 eV and (b) 30 eV with the 0.024 nm fwhm resolution.

higher pressures, secondary electron effects on formation of $N_2(C)$ become serious above 30 eV, especially in the cases where magnetic collimation was used. In the present experiment, the ambient pressure at the collision chamber was 3 to 5 times as high as the critical pressure at which secondary electron effects cannot be disregarded. On the other hand, secondary electron effects on formation of $N_2^+(B)$ are insignificant under the present experimental conditions. Thus, the secondary electron effects were estimated on comparing the emission cross sections (ECS) of the $N_2(C–B)$ band with those of the $N_2^+(B–X)$ band. Figure 5 shows the ECS of the $N_2(C–B)$ band, $\sigma(C–B)$, relative to that of the $N_2^+(B–X)$ band, $\sigma(B–X)$; the observed ratios are normalized to the ratio at 20 eV calculated from the published ECSs[28,29] on the assumption that the secondary electron effects are negligible below 20 eV. The present values above 25 eV deviate from the ratios evaluated from the published ECSs.[28,29] The contribution of secondary electrons to formation of $N_2(C)$ is estimated to be 39% at 25 eV, 64% at 30 eV, and 86% at 60 eV on comparing the observed ratios with the calculated ratios. Thus, secondary electron effects on formation of $N_2(C)$ increase with the impact energy and become

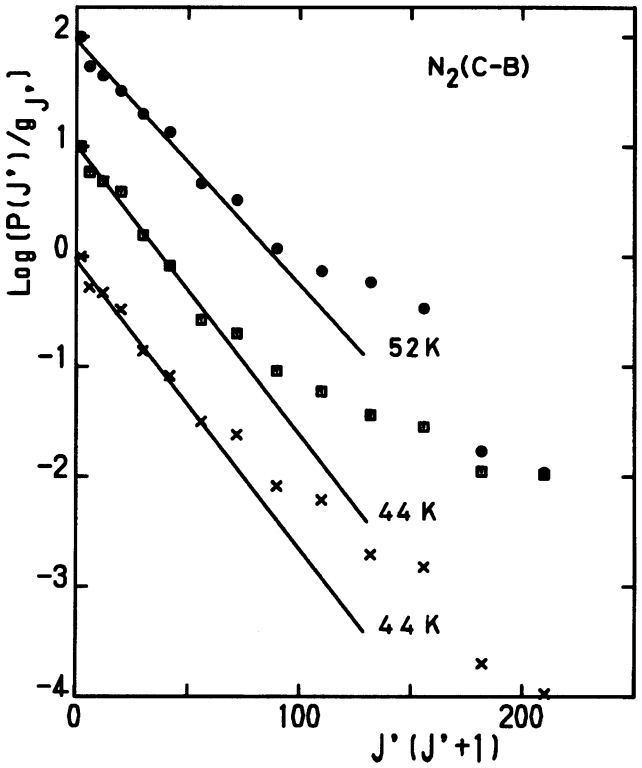


Fig. 3. Logarithmic plots of $P(J')/g_{J'}$ versus $J'(J'+1)$ for $N_2(C)$ obtained at impact energies of () 14 eV, (□) 20 eV, and (×) 30 eV: The $P(J'=1)$ values of 14, 20, 30 eV are normalized to 100, 10, 1, respectively, for clarity.

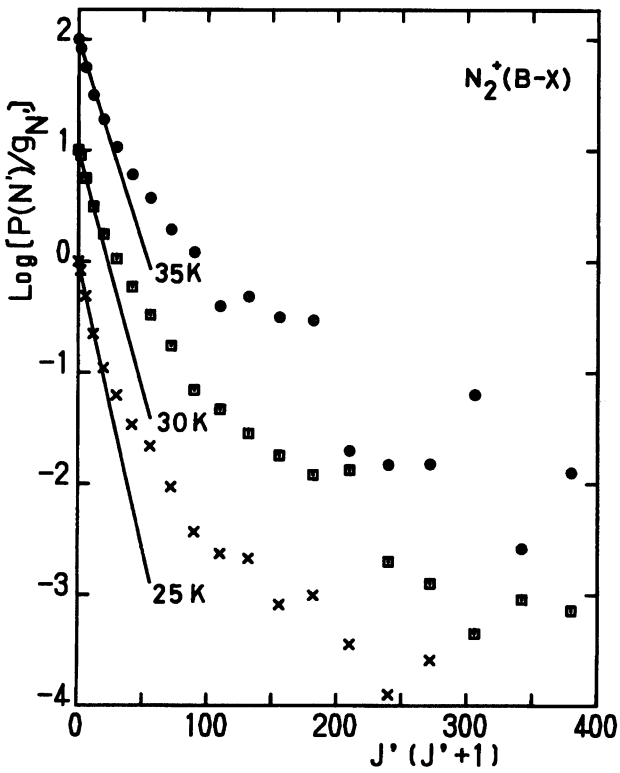


Fig. 4. Logarithmic plots of $P(N')/g_{N'}$ versus $N'(N'+1)$ for $N_2^+(B)$ obtained at impact energies of () 30 eV, (□) 45 eV, and (×) 100 eV: The $P(N'=0)$ values of 30, 45, 100 eV are normalized to 100, 10, 1, respectively, for clarify.

serious above 25 eV. This effect will be discussed later.

**Deviation from Boltzmann Distribution.** The rotational distributions of the $N_2(C)$ and $N_2^+(B)$ states are non-Boltzmann as shown in Figs. 3 and 4; the populations for $J'$ above 8 of $N_2(C)$ are enhanced than those extrapolated from the lower levels, and the populations for $N'$ above 5 of $N_2^+(B)$ are also enhanced. These deviations from a single Boltzmann distribution probably originate in either the rotational excitation or the non-Boltzmann distribution of initial target molecules in free jet. Although large changes in rotational quantum number, $|\Delta J| \geqq 2$, through multipole interactions can overpopulate the product state at higher rotational levels,[4] it is important to measure the initial rotational distribution and to examine whether the target molecules in the free jet are rotationally in equilibrium or not. Unfortunately, the initial rotational distributions of target $N_2$ could only be estimated roughly as described below.

Marrone[2] and Ashkenas[3] observed that the rotational distributions of $N_2^+(B)$ are non-Boltzmann and lag from a temperature calculated from the isentropic flow equations. The degree of departure from the isentropic condition was found to depend on the Reynolds number.[2] Polanyi and Woodall[30] pointed out that the probability of rotational to translational energy transfer decreases with increasing the rotational quantum number. Thus, the deviation from a Boltzmann distribution observed seems to be caused by the circumstance that the isentropic condition is not realized in the present experimental conditions. This conclusion is however not necessarily to disregard the contribution of rotational excitation. The present study does not answer the origin of the deviation.

**Rotational Excitation.** The rotational distributions observed for the $N_2(C)$ and $N_2^+(B)$ states are found to be non-Boltzmann. Therefore, it is convenient to introduce a parameter which can represent the rotational distribution. In the circumstances, the rotational distribution is converted to the average rotational energy ($E_R$) and the average rotational quantum number ($\bar{J}'$ or $\bar{N}'$) for comparison with the other data. In the present study, the rotational energy of the $N_2(C)$ state is defined by

$$E_R = \frac{\Sigma hcF(J')P(J')}{\Sigma P(J')}, \tag{3}$$

where $F(J')$ is the rotational term value, and the summations are taken over $J'$ up to 14. The average rotational quantum number $\bar{J}'$ is given by

$$\bar{J}' = \frac{\Sigma J'P(J')}{\Sigma P(J')}. \tag{4}$$

For $N_2^+(B)$, the average rotational energy and the average rotational quantum number are also given by Eqs. 3

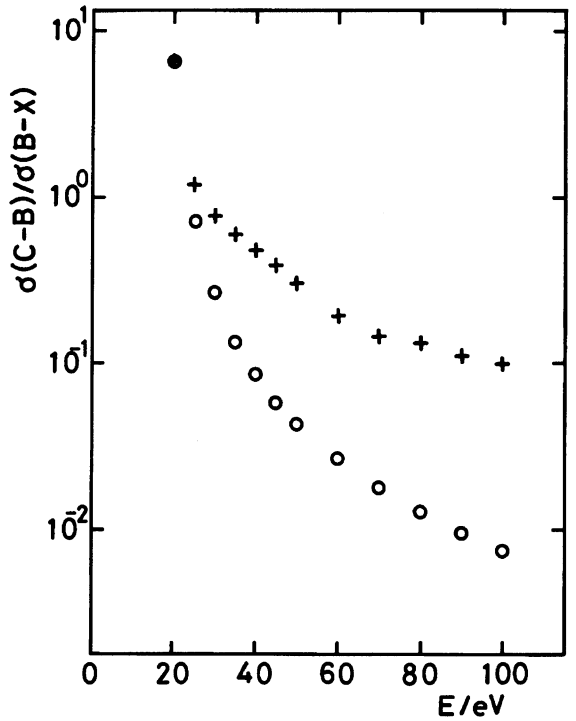


Fig. 5. Ratios of the ECS of the $N_2$(C–B) band to that of the $N_2^+$(B–X) band: (×) the present results, (○) the values calculated from the ECSs adopted from Refs. 28 and 29.

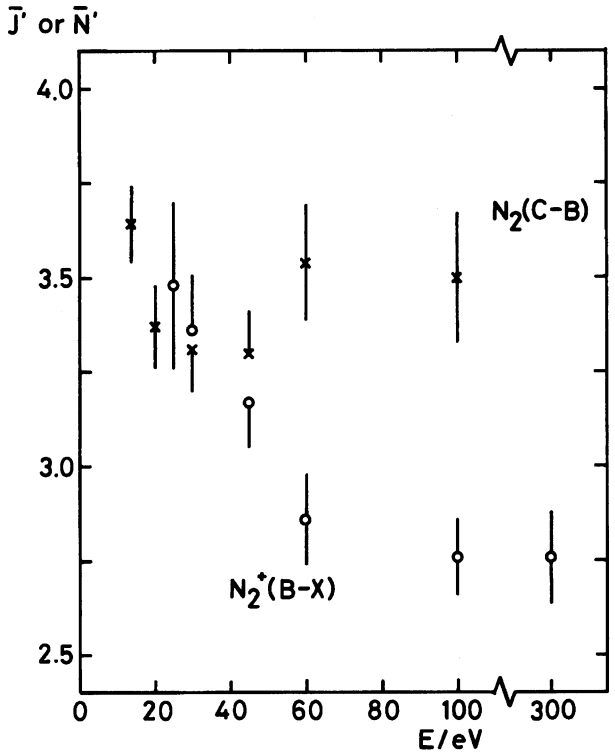


Fig. 6. Average rotational quantum numbers versus impact energy: (×) $\overline{J}'$ for $N_2$(C), (○) $\overline{N}'$ for $N_2^+$(B).

and 4 with replacing $J'$ with $N'$ and summing over $N'$ up to 19.

The values of the rotational energy and the average rotational quantum number for $N_2$(C) and $N_2^+$(B) thus obtained are listed in Table 1 comparing with those for $N_2^+$(X).[14,16] The dependences of $\overline{J}'$ and $\overline{N}'$ on the impact energy are displayed in Fig. 6. The $\overline{N}'$ values for $N_2^+$(B) are very similar to those for $N_2^+$(X), whereas the $E_R$ values for $N_2^+$(B) are considerably larger than those for $N_2^+$(X). This difference is due to the statistical weight resulting from the presence of nuclear spin; for $N_2$ the symmetric rotational levels occur twice those for the asymmetric levels.

The rotational excitation of the product states should reflect the selection rules for rotational transitions. Therefore, it is convenient to use the average rotational quantum number instead of the rotational energy in order to understand the interactions operating in excitation and ionization. First, we discuss the rotational excitation observed for $N_2^+$(B) since its trend has been investigated in details,[4—6] and then we consider the trend in $N_2$(C).

The $\overline{N}'$ values of the $N_2^+$(X) and $N_2^+$(B) ions enhance rapidly with decreasing impact energy as shown in Table 1. In electron-impact ionization, an incident electron is scattered by a target molecule and then the excited molecule ejects an electron. The rotational transition can be postulated qualitatively by a two-step model:[5] (a) the first step is due to the interactions between the incident electron and the neutral target; (b) the interaction between the scattered and ejected electrons and the residual ion causes the pure rotational excitation in the second step. In the limit of high electron energy, the rotational excitation takes place only by the interaction between the ejected electron and the product ion.[14] Interactions in step (b) become unimportant near the ionization threshold and then the rotational excitation is primary due to the electron-multipole interactions of step (a).[14] Nevertheless, neither step (a) nor step (b) is completely applicable in the electron energy range of the 14—300 eV. At such an intermediate electron energy, both interactions can contribute to the rotational excitation.

The rotational transitions allowed for formation of $N_2^+$(B) are displayed in Fig. 7. When the Born approximation is applied to interactions in step (a), the rotational transitions in the $N_2(X^1\Sigma_g^+)$—$N_2^+(B^2\Sigma_u^+)$ ionization-excitation must obey the selection rule, $|\Delta N|=1$, 3, ⋯, to satisfy conservation of nuclear symmetry. In contrast, the leading term of interactions in step (b) corresponds the quadrupole moments of $N_2^+$(B),[17] so that the rotational transitions of the $N_2^+$(B) states in step (b) must obey the selection rule, $|\Delta N|=0$ and 2.

The $\overline{N}'$ values for $N_2^+$(B) were evaluated to be 3.5 at 25 eV and 2.8 at 300 eV. Thus, the $N_2^+$(B) ions produced at 25 eV gain an angular momentum of 0.7 $h/2\pi$ in excess of that of the ions produced at 300 eV. The net increase in the average rotational quantum number $\Delta\overline{N}'$ from 300 to 30 eV is a half of the value of 1.5

Table 1. Degrees of Rotational Excitation in $N_2(C^3\Pi_u)$, $N_2^+(B^2\Sigma_u^+)$, and $N_2^+(X^2\Sigma_g^+)$ Produced by Electron Impact on $N_2$ [a]

| $E$/eV | $N_2(C^3\Pi_u)$ | | $N_2^+(B^2\Sigma_u^+)$ | | $N_2^+(X^2\Sigma_g^+)$ | |
|---|---|---|---|---|---|---|
| | $E_R$/meV | $\overline{J'}$ | $E_R$/meV | $\overline{N'}$ | $E_R$/meV | $\overline{N''}$ |
| 14 | 5.0(3) | 3.64(10) | | | | |
| 20 | 4.4(2) | 3.37(11) | | | | |
| 25 | | | 5.4(8) | 3.48(22) | 4.3(2)[b] | 4.2(2)[b] |
| 30 | 4.3(2) | 3.31(11) | 4.8(2) | 3.36(15) | 4.2(2)[b] | 3.9(2)[b] |
| 45 | 4.3(3) | 3.30(11) | 4.5(3) | 3.17(12) | 3.6(1)[c] | 3.4(1)[d] |
| 60 | 4.9(3) | 3.54(15) | 3.6(3) | 2.86(12) | 3.5(1)[c] | 3.3(1)[d] |
| 100 | 4.8(3) | 3.50(17) | 3.5(4) | 2.76(10) | 2.6(1)[c] | 2.8(1)[d] |
| 300 | | | 3.7(4) | 2.76(12) | 2.3(2)[c] | 2.7(2)[d] |

a) Numbers in parentheses mean absolute errors attached to the last digit. b) Estimated from Fig. 5 in Ref. 14. c) From Ref. 14. d) From Ref. 16.

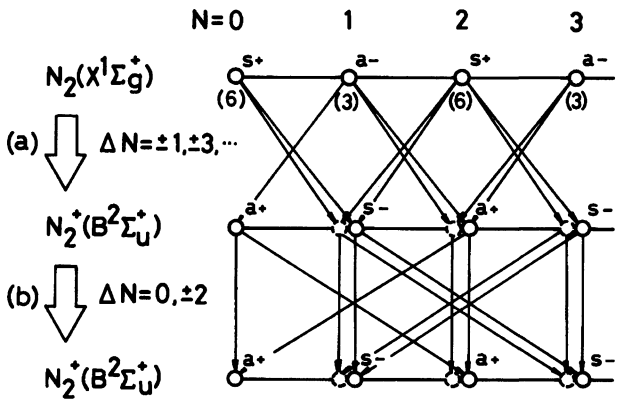


Fig. 7. Schematic diagrams of rotational transitions for $N_2^+(B)$: (a) rotational transitions with $\Delta N=\pm1$, $\pm3$, $\cdots$ are allowed in the ionization-excitation step $[N_2\rightarrow N_2^+(B^2\Sigma_u^+)+e]$, but the $\Delta N=\pm1$ transitions only are displayed; (b) the quadrupole transitions ($\Delta N=0$, $\pm2$) are allowed in pure rotational step.

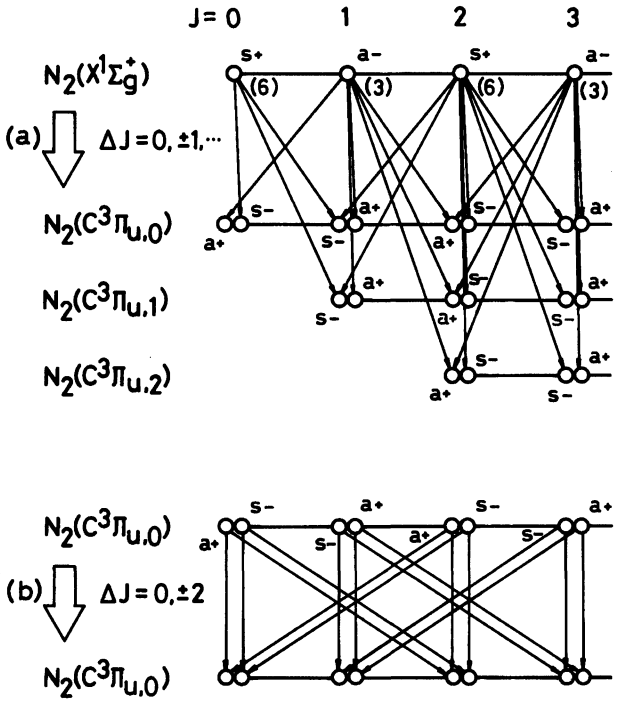


Fig. 8. Schematic diagrams of rotational transitions for $N_2(C)$: (a) all rotational transitions are allowed in the excitation step $[N_2\rightarrow N_2(C^3\Pi_u)]$, but the $\Delta N=0$ and $\pm1$ transitions only are displayed; (b) the quadrupole transitions with $\Delta J=0$, $\pm2$ are allowed in the pure rotational step.

obtained for $N_2^+(X)$. This difference is probably caused by the selection rule in step (a) since the selection rule in the $N_2(X^1\Sigma_g^+)$—$N_2^+(X^2\Sigma_g^+)$ ionization-excitation is $|\Delta N|=0$, 2, $\cdots$ to satisfy conservation of nuclear symmetry in contrast to the selection rule, $|\Delta N|=1$, 3, $\cdots$, in step (a) for $N_2^+(B)$. For step (b), the selection rule of $N_2^+(X)$ is the same as that of $N_2^+(B)$. Moreover, step (b) becomes insignificant at low impact energy.[14]

Now, we consider the rotational excitation in $N_2(C)$. Formation of $C^3\Pi_u$ from the $X^1\Sigma_g^+$ state of $N_2$ is a spin-forbidden type. Nevertheless, the $N_2(C^3\Pi_u)$ state is produced in electron impact via an electron exchange process between the incident electron and the valence electron. The rotational transitions in the $N_2(X^1\Sigma_g^+$—$C^3\Pi_u)$ excitation are all allowed, $|\Delta J|=0$, 1, 2, $\cdots$, whereas those in step (b) must obey the selection rule, $|\Delta J|=0$ and 2, as displayed in Fig. 8.

The $\overline{J'}$ value for $N_2(C)$ decreases with increasing the impact energy up to 30 eV, reaches a minimum, increases above 45 eV, and reaches a constant. The trend of rotational excitation below 30 eV for $N_2(C)$ is found for the first time. The increase above 45 eV is probably due to secondary electron effects on formation of $N_2(C)$ as discussed previously since the rotational distribution is enhanced much more effectively by collisions of target molecules with slow electrons. If we can remove the secondary electron effects, the $\overline{J'}$ values are expected to decrease with increasing the impact energy in much wider range.

The net increase in the average rotational quantum number $\Delta\overline{J'}$ for $N_2(C)$ from 9 eV above the threshold (11.0 eV) to 3 eV above the threshold is 0.3. The $\Delta\overline{N'}$ value for $N_2^+(B)$ from 11 eV above the threshold (18.8 eV) to 6 eV above the threshold is 0.1, while that for

$N_2^+(X)$ from 14 eV above the threshold (15.6 eV) to 9 eV above the threshold is 0.3. Since the rotational excitation is effective near the threshold, the rotational enhancement in $N_2(C)$ seems to be larger than that in $N_2^+(B)$ but is smaller than that in $N_2^+(X)$.

The order of rotational excitation among these states is mainly ascribed to interactions in step (a), while the contribution of the interactions in step (b) seems to be insignificant since the selection rule in step (b) is the same for $N_2(C)$, $N_2^+(X)$, and $N_2^+(B)$, and since the interactions resulting from quadrupole moments of these states are expected to be small. Moreover, step (b) becomes insignificant near the threshold. Thus, it is concluded that multipole interactions and the rotational selection rule at step (a) seem to be important in rotational excitation in formation of these states. This conclusion, however, is inconsistent with that obtained for the triatomic $N_2O^+(\tilde{A})$, $CO_2^+(\tilde{A})$, and $CS_2^+(\tilde{A})$ ions;[18] for the triatomic ions, it is concluded that the quadrupole interaction at step (b) is important. This discrepancy is probably ascribed to the difference in the magnitude of the quadrupole moment and in the impact energy range; we have not succeeded in the measurement at the impact energy below 30 eV for the triatomic ions.

## References


1) F. Robben and L. Talbot, *Phys. Fluids*, **9**, 644 (1966).
2) P. V. Marrone, *Phys. Fluids*, **10**, 521 (1967).
3) H. Ashkenas, *Phys. Fluids*, **10**, 2509 (1967).
4) D. Coe, F. Robben, L. Talbot, and R. Cattolica, *Phys. Fluids*, **23**, 706 (1980).
5) B. M. Dekoven, D. H. Levy, H. H. Harris, B. R. Zegarski, and T. A. Miller, *J. Chem. Phys.*, **74**, 5659 (1981).
6) S. P. Hernandez, P. J. Dagdigian, and J. P. Doering, *Chem. Phys. Lett.*, **91**, 409 (1982); *J. Chem. Phys.*, **77**, 6021 (1982).
7) A. E. Kassem and R. S. Hickman, *Phys. Fluids*, **17**, 1976 (1974).
8) H. Helvajian, B. M. Dekoven, and A. P. Baronavski, *Chem. Phys.*, **90**, 175 (1984).
9) P. J. Dagdigian and J. P. Doering, *Chem. Phys.*, **104**, 355 (1986).
10) P. J. Dagdigian and J. P. Doering, *J. Chem. Phys.*, **78**, 1846 (1983).
11) J. Allison, T. Kondow, and R. N. Zare, *Chem. Phys. Lett.*, **64**, 202 (1979).
12) M. I. Lester, B. R. Zegarski, and T. A. Miller, *J. Phys. Chem.*, **87**, 5228 (1983).
13) H. Kawazumi, T. Uchida, and T. Ogawa, *Bull. Chem. Soc. Jpn.*, **59**, 937 (1986)
14) T. Nagata, A. Nakajima, T. Kondow, and K. Kuchitsu, *J. Chem. Phys.*, **87**, 6507 (1987).
15) P. W. Zetner, M. Darrach, P. Hammond, W. B. Westerveld, R. L. McConkey, and J. W. McConkey, *Chem. Phys.*, **124**, 453 (1988).
16) A. Nakajima, T. Nagata, T. Kondow, and K. Kuchitsu, *Chem. Phys. Lett.*, **151**, 511 (1988).
17) E. Gerjuoy and S. Stein, *Phys. Rev.*, **97**, 1671 (1955); **98**, 1848 (1955).
18) I. Tokue, A. Masuda, H. Kume, and Y. Ito, *Chem. Phys.*, **158**, 161 (1991).
19) I. Tokue, H. Shimada, A. Masuda, Y. Ito, and H. Kume, *J. Chem. Phys.*, **93**, 4812 (1990).
20) K. P. Huber and G. Herzberg, "Molecular Spectra and Molecular Structure," "Vol.**4**, Constants of Diatomic Molecules," Van Nostr and Reinhold, New York (1979).
21) G. Hertzberg, "Molecular Spectra and Molecular Structure," "Vol. **1**, Spectra of Diatomic Molecules," Van Nostr and Reinhold, New York (1950).
22) A. Budó, *Z. Phys.*, **105**, 579 (1937).
23) D. Coster, F. Brons, and A. van der Ziel, *Z. Phys.*, **84**, 304 (1933).
24) A. Guntsch, *Z. Phys.*, **86**, 262 (1933).
25) D. Coster and H. H. Brons, *Z. Phys.*, **73**, 747 (1932).
26) D. M. Lubman, C. T. Rettner, and R. N. Zare, *J. Phys. Chem.*, **86**, 1129 (1982).
27) W. L. Borst and M. Imami, *J. Appl. Phys.*, **44**, 1133 (1972).
28) M. Imami and W. L. Borst, *J. Chem. Phys.*, **61**, 1115 (1974).
29) W. L. Borst and E. C. Zipf, *Phys. Rev. A*, **3**, 834 (1970).
30) J. C. Polanyi and K. B. Woodall, *J. Chem. Phys.*, **56**, 1563 (1972).